Acta Pharmacologica Sinica

www.nature.com/aps

ARTICLE

10,11-dehydrocurvularin exerts antitumor effect against human breast cancer by suppressing STAT3 activation

Qun Zhao[1], Yun Bi[1], Jing Zhong[1,2], Xiang Li[1], Jian Guo[1], Ying-xiang Liu[1], Long-rui Pan[1], Yan Tan[1], Zhang-shuang Deng[2] and Xian-jun Yu[1]

Aberrant activation of signal transducer and activator of transcription 3 (STAT3) plays a critical role in many types of cancers. As a result, STAT3 has been identified as a potential target for cancer therapy. In this study we identified 10,11-dehydrocurvularin (DCV), a natural-product macrolide derived from marine fungus, as a selective STAT3 inhibitor. We showed that DCV (2–8 μM) dose-dependently inhibited the proliferation, migration and invasion of human breast cancer cell lines MDA-MB-231 and MDA-MB-468, and induced cell apoptosis. In the two breast cancer cell lines, DCV selectively inhibited the phosphorylation of STAT3 Tyr-705, but did not affect the upstream components JAK1 and JAK2, as well as dephosphorylation of STAT3. Furthermore, DCV treatment strongly inhibited IFN-γ-induced STAT3 phosphorylation but had no significant effect on IFN-γ-induced STAT1 and STAT5 phosphorylation in the two breast cancer cell lines. We demonstrated that the α, β-unsaturated carbonyl moiety of DCV was essential for STAT3 inactivation. Cellular thermal shift assay (CETSA) further revealed the direct engagement of DCV with STAT3. In nude mice bearing breast cancer cell line MDA-MB-231 xenografts, treatment with DCV (30 mg·kg^{-1}·d^{-1}, ip, for 14 days) markedly suppressed the tumor growth via inhibition of STAT3 activation without observed toxicity. Our results demonstrate that DCV acts as a selective STAT3 inhibitor for breast cancer intervention.

Keywords: breast cancer; STAT3; 10,11-dehydrocurvularin; cellular thermal shift assay; MDA-MB-231 cells; MDA-MB-468 cells; tumor growth

Acta Pharmacologica Sinica (2021) 42:791–800; https://doi.org/10.1038/s41401-020-0499-y

INTRODUCTION

Breast cancer is the most common tumor in women, and ~400,000 breast cancer-related deaths are recorded annually worldwide [1, 2]. Although advanced therapies are available to treat breast cancer, the prognosis of patients is still poor, mainly because of widespread metastasis and high recurrence rates [3, 4]. Chemotherapy has become a promising strategy for breast cancer treatment; however, it also has some undesirable side effects [5, 6]. Thus, there is an urgent need to develop a novel therapeutic strategy for breast cancer to improve the clinical outcome of patients.

Signal transducer and activator of transcription 3 (STAT3) is an important transcription factor in normal tissue development and involution [7, 8]. In normal cells, STAT3 is expressed as an inactive monomer in the cytoplasm. Cytokines, such as IL-6 and other growth factors, can induce dimerization of the gp130 receptor and activation of the receptor-associated JAK kinases, leading to phosphorylation of STAT3 [9, 10]. Phosphorylated STAT3 forms dimers and subsequently enters the nucleus and regulates the transcription of target genes [11]. Constitutive activation of the STAT3 signaling pathway contributes to tumor development and progression in various cancers [12, 13]. With respect to breast cancer, constitutive activation of STAT3 is strongly associated with the prognosis of breast cancer and is found in more than 40% of breast cancer cases [14]. Previous studies have shown that aberrant and constitutively activated STAT3 is linked with proliferation [15], apoptosis [16], metastasis [17, 18], and chemoresistance [19, 20] in breast cancer. Pharmacologic suppression of STAT3 activation has been revealed as a novel therapeutic strategy for the treatment of breast cancer [21–25]. Therefore, STAT3 is deemed an attractive target for therapeutic intervention in breast cancer.

10,11-dehydrocurvularin (DCV), a fungus-derived natural-product macrolide exhibits anti-infective, anti-inflammatory, and anticancer activities [26–30]. However, the detailed molecular mechanisms of DCV remain elusive. Given the critical role of STAT3 in the development of cancer and the anticancer potential of DCV, we postulated that DCV exerts anticancer effects through the modulation of STAT3 activation. In this study, we report that DCV potently inhibits STAT3 activation in vitro and in vivo. We found that the Michael acceptor moiety on DCV is responsible for the inhibition of STAT3 activation. In conclusion, these results imply that DCV exerts anticancer activity in breast cancer by suppressing STAT3 signaling.

[1]Laboratory of Inflammation and Molecular Pharmacology, School of Basic Medical Sciences & Biomedical Research Institute, Hubei University of Medicine, Hubei Key Laboratory of Embryonic Stem Cell Research, Hubei Key Laboratory of Wudang Local Chinese Medicine Research, Hubei University of Medicine, Shiyan 442000, China and [2]Hubei Key Laboratory of Natural Products Research and Development, China Three Gorges University, Yichang 443002, China
Correspondence: Zhang-shuang Deng (dzs163@163.com) or Xian-jun Yu (xjyu@hbmu.edu.cn)
These authors contributed equally: Qun Zhao, Yun Bi

Received: 8 March 2020 Accepted: 29 June 2020
Published online: 31 August 2020

MATERIALS AND METHODS

Reagents and antibodies

DCV and curvularin (CV) have been previously described [26, 30]. DCV and CV were dissolved in dimethyl sulfoxide DMSO (Amresco, Cleveland, OH, USA) at 20 mM to generate stock solutions. Antibodies for Western blotting used in this study included rabbit anti-PARP (#9532, Cell Signaling Technology, Beverly, MA, USA; 1:1000), rabbit anti-cleaved caspase-3 (#9661), rabbit anti-Bcl-2 (#3498), rabbit anti-Bax (#2772), rabbit anti-phospho-STAT3 (Tyr705) (#9145), rabbit anti-phospho-STAT3 Ser727 (#9134), mouse anti-phospho-STAT3 (#9139), rabbit anti-phospho-STAT1 (#7649), rabbit anti-STAT1 (#9172), rabbit anti-phospho-STAT5 (#9314), rabbit anti-STAT5 (#94205), rabbit anti-phospho-JAK1 (#3331), rabbit anti-JAK1 (#3332), rabbit anti-phospho-JAK2 (#3776), rabbit anti-JAK2 (#3230). Flag-beads (#A2220, Sigma, St. Louis, MO, USA), Flag (#A8592, Sigma, St. Louis, MO, USA; 1:1000) and β-actin (#A3854, Sigma, St. Louis, MO, USA; 1:5000) were also used in this study.

Cell line and culture

Human breast cancer cell lines (MDA-MB-231 and MDA-MB-468) and normal breast epithelial cells (MCF-10A) were provided by Prof Tao Zhu at the University of Science and Technology of China, Hefei, Anhui, China [31]. Human embryonic kidney HEK293T cells were purchased from the Cell Bank of the Chinese Academy of Sciences (Shanghai, China). MDA-MB-231, MDA-MB-468, and HEK293T cells were cultured in Dulbecco's modified Eagle's medium (DMEM, Gibco; Thermo Fisher Scientific, Inc., Waltham, MA, USA) supplemented with 10% fetal bovine serum (FBS, Biological Industries, Israel), 100 U/mL penicillin, and 100 μg/mL streptomycin (Thermo Fisher Scientific, Inc., Waltham, MA, USA). MCF-10A cells were maintained in DMEM/F12 medium (Gibco; Thermo Fisher Scientific, Inc., Waltham, MA, USA) containing 5% horse serum (HS), insulin (10 mg/mL), epidermal growth factor (EGF, 20 ng/mL), cholera toxin (100 mg/mL), hydrocortisone (0.5 mg/mL), penicillin (50 U/mL), and streptomycin (50 U/mL) (obtained from PeproTech; Rocky Hill, NJ, USA). All cells were maintained in a humidified 5% CO_2 incubator at 37 °C.

Cell viability assay

Cells were seeded in 96-well microplates (5×10^4 cells/well) and cultured for 24 h. The cells were treated with a series of concentrations of compounds for the indicated periods. Cell viability was determined by MTT assay in triplicate [32].

Colony formation assay

Cells were pretreated with the indicated concentrations of DCV for 12 h and then cultured in DMEM containing 10% FBS. After 14 days, the colonies were stained with 0.1% crystal violet and quantified under a light microscope.

Cell apoptosis assay

Cells were resuspended in 1× binding buffer and then incubated with annexin V and propidium iodide (PI) for 30 min in the dark at room temperature, after which the number of apoptotic cells was analyzed by flow cytometry.

Wound-healing migration assay

Cells (5×10^5) were seeded in a six-well plate after reaching confluence. Cells were scratched with a 200 μL pipet tip and then washed with PBS to remove unattached cells. The cells were treated with the indicated concentrations of DCV in DMEM containing 10% FBS. After 12 h of incubation, the cells were fixed, and randomly chosen fields were imaged under a light microscope.

Invasion assay

The invasion assay was carried out using a coated polyvinyl-pyrrolidone-free polycarbonate filter (Corning). Cells (2×10^4 cells/well) were resuspended in medium with or without the indicated concentrations of DCV and added to the Transwell insert. Complete medium was added to the bottom well. Twelve hours after seeding, the filter was fixed and stained with 2% ethanol containing 0.2% crystal violet (15 min). After being dried, the stained cells were counted under a light microscope.

Luciferase reporter assay

The STAT3 luciferase reporter plasmid pAPRE-luc (containing the STAT3 responsive element) was used to detect the transcriptional activity of STAT3 signaling and was a gift from Professor Guang-biao Zhou. The assay was carried out as previously described [33]. Briefly, cells were cotransfected with the STAT3 luciferase reporter plasmid and SV40-Renilla-Luc (Promega, Madison, WI, USA) using Lipofectamine 2000 (Invitrogen, USA) for 24 h. Then, the cells were pretreated with DCV for 2 h, and IL-6 (R&D Systems, Minneapolis, MN, USA, 10 ng/mL) was added and incubated for an additional 24 h. Luciferase activity was detected using the Dual-Luciferase Reporter Assay System (Promega, Madison, WI, USA), and the relative reporter activity was obtained by normalizing to the Renilla luciferase activity according to the manufacturer's instructions.

Western blotting

Cells and tissues were harvested and lysed in RIPA buffer (containing protease and phosphatase inhibitor cocktail) for 30 min on ice. After centrifugation, protein samples were quantified using a BCA protein assay kit (#P0011, Beyotime Institute of Biotechnology, Shanghai, China). Equal amounts of proteins were loaded onto SDS-PAGE gels at 100 V for 2 h and transferred to PVDF membranes (Millipore, Plano, TX, USA). The membranes were further blocked with 5% nonfat milk and incubated with primary antibodies at 4 °C overnight. The membranes were further incubated with HRP-conjugated secondary antibodies for 1 h at room temperature and then detected by a chemiluminescence kit (Millipore, Plano, TX, USA).

Isolation of cytosolic and nuclear extracts

Cells were treated with DCV for 2 h, followed by 20 min of stimulation with IL-6 (10 ng/mL, and cytosolic and nuclear extracts were isolated using a nuclear extraction kit (#P0027, Beyotime Biotechnology, Shanghai, China) according to the manufacturer's instructions. The extracts were quantified using the BCA assay.

Cellular thermal shift assay (CETSA)

CETSA was performed as previously described [30]. Briefly, MDA-MB-231 and MDA-MB-468 cells were treated with or without 6 μM DCV for 2 h. Cells were washed with PBS and suspended in 1 mL PBS (containing protease and phosphatase inhibitor cocktail) and then divided into five PCR tubes. The tubes were heated at the indicated temperatures for 3 min, followed immediately by cooling on ice. The cells were lysed via three freeze (in dry ice)-thaw (in 25 °C water bath) cycles. The cell lysates were centrifuged at $20{,}000 \times g$ for 20 min at 4 °C. Soluble supernatants were analyzed by gel electrophoresis and Western blotting.

Coimmunoprecipitation assay

Cells were collected with NP40 cell lysis buffer, and the protein samples were incubated with the indicated antibodies overnight at 4 °C. Then, immunoprecipitates were incubated with protein A/G agarose beads for 2 h at 4 °C. Protein expression was detected by Western blotting.

Tumor xenografts in nude mice

Female BALB/c-nu mice (Beijing HuaFuKang Bioscience Co., Ltd, Beijing, China) were purchased at 4–5 weeks of age and housed in a specific pathogen-free barrier facility. MDA-MB-231 cells (1×10^6) in 100 μL PBS were subcutaneously injected into the right flanks of mice. When the tumors were visible, the mice were randomly divided into two groups (seven mice in each group): the vehicle

group and the DCV (30 mg·kg^{-1}·d^{-1}) group. The mice in the vehicle group were injected intraperitoneally with 100 μL 95% PBS + 5% Cremophor daily, while the mice in the DCV group were injected with DCV diluted with 95% PBS + 5% Cremophor (30 mg·kg^{-1}·d^{-1}). Body weights were monitored. The tumor size was measured using slide calipers, and the tumor volume was calculated as $0.5 \times a \times b^2$, where a is the length of the tumor, and b is the width. At the time of the last treatment, the mice were euthanized. The tumors were excised and weighed and then frozen immediately in liquid nitrogen for further analysis.

Statistical analysis

All data represent at least three independent experiments and are expressed as the mean ± standard deviation unless otherwise noted. An unpaired *t* test was performed to compare two samples to determine the statistical significance of the difference. $P < 0.05$ was considered to represent a statistically significant difference.

Ethical statement

All animal experiments were performed in accordance with the guidelines for animal treatment of Hubei University of Medicine. All experimental protocols in our study were approved by the Ethics Committee of Hubei University of Medicine.

RESULTS

Inhibitory effects of DCV on breast cancer cells

To investigate the potential cell growth inhibitory effects of DCV (Fig. 1a) in breast cancer cells, we first assessed the effect of DCV on MDA-MB-231 and MDA-MB-468 cells. As shown in Fig. 1b, DCV inhibited cell proliferation in both cancer cell lines in a concentration- and time-dependent manner. However, the normal human mammary epithelial cell line MCF-10A was less sensitive to DCV (Fig. 1c). To further confirm the antiproliferative effect of DCV, we performed a cell clonogenic assay. DCV significantly reduced the clonogenic activity in the two cell lines (Fig. 1d). We next examined whether DCV inhibited migration and invasion. The migration and invasion of cells were effectively impaired by DCV in a concentration-dependent manner (Fig. 1e, f). We then investigated the apoptotic response to DCV treatment. DCV treatment increased the proportion of annexin V/PI-positive cells according to the flow cytometry analysis (Fig. 1g). In agreement with the above findings, the levels of cleaved PARP and caspase-3 were significantly increased by DCV treatment in a concentration-dependent manner (Fig. 1h). As further confirmation that DCV-induced apoptosis in breast cancer cells, the results showed upregulation of Bax and downregulation of Bcl-2 after exposure to DCV (Fig. 1i). Collectively, these results indicate that DCV exhibits anticancer activity in human breast cancer cells in vitro.

DCV specifically inhibits STAT3 activation

STAT3 is a transcription factor whose aberrant constitutive activation contributes to cell growth and metastasis [34]. We assessed whether DCV suppressed the transcriptional activation of STAT3. A STAT3-responsive luciferase reporter assay system was used to identify STAT3 signaling inhibitors [33]. We found that DCV inhibited STAT3-responsive luciferase activity in a concentration-dependent manner (Fig. 2a). Moreover, DCV also significantly suppressed IL-6-induced STAT3-responsive luciferase activity (Fig. 2b). To determine whether STAT3 was activated, we examined the phosphorylation of STAT3 in MDA-MB-231 and MDA-MB-468 cells by Western blotting. The results showed that DCV inhibited constitutive STAT3 phosphorylation at Tyr705 in a concentration-dependent manner but did not affect STAT3 phosphorylation at Ser727 (Fig. 2c). DCV also exerted similar inhibitory effects on IL-6-induced STAT3 phosphorylation in a concentration- and time-dependent manner (Fig. 2d, e). In addition, compared with the STAT3 selective inhibitors cryptotanshinone and BP-1-102, DCV showed a strong inhibitory effect on STAT3 phosphorylation (Fig. S1).

One essential step for STAT3 activation is the nuclear translocation of STAT3, which is critical for subsequent target gene regulation [12]. To further confirm the inhibitory effect of DCV on STAT3 activation, we examined the effects of DCV on STAT3 nuclear translocation and target gene expression. DCV markedly inhibited IL-6-induced nuclear translocation of STAT3 in the two breast cancer cell lines, as demonstrated by cytoplasmic and nuclear fractionation (Fig. 2f). Furthermore, DCV significantly inhibited the expression of the STAT3 target genes Cyclin D1, survivin, and c-Myc in a concentration-dependent manner (Fig. 2g).

STAT1 and STAT5 are structurally similar to STAT3 but have different functions [35, 36]. To determine whether DCV is a STAT3-specific inhibitor, MDA-MB-231 and MDA-MB-468 cells were stimulated with IFN-γ, and the effect of DCV was examined. Interestingly, DCV strongly suppressed IFN-γ-induced STAT3 phosphorylation but had no significant effect on IFN-γ-induced STAT1 or STAT5 phosphorylation (Fig. 2h), implying that DCV specifically inhibits STAT3 phosphorylation. Therefore, these results indicate that DCV inhibits STAT3 activation in human breast cancer cells.

DCV does not affect the upstream components or dephosphorylation of STAT3

The binding of the cytokine IL-6 to its receptor initiates the activation of STAT3 upstream receptor-associated kinases, which then activate STAT3. To explore whether DCV directly interacts with IL-6, we incubated IL-6 with DCV. We observed that incubation of IL-6 with DCV maintained the high expression of STAT3 phosphorylation, implying that DCV does not directly interact with IL-6 (Fig. 3a, b). Receptor-associated kinases, such as JAK1 and JAK2, are the upstream kinases of STAT3. We then examined whether STAT3 inhibition by DCV occurred through inhibition of JAK1 and JAK2. DCV had no effects on the constitutive phosphorylation of JAK1 and JAK2 (Fig. 3c). Moreover, DCV did not inhibit the IL-6-induced phosphorylation of JAK1 and JAK2 (Fig. 3d). These results suggest that inhibition of STAT3 by DCV is not mediated by inhibition of its upstream receptor-associated kinases.

Protein tyrosine phosphatases (PTPs) have been implicated in STAT3 activation. We assessed whether the DCV-induced inhibition of STAT3 phosphorylation could be due to the activation of PTPs. Cells were stimulated with IL-6 and cultured in fresh medium for the indicated time points, after which STAT3 phosphorylation was detected. Treatment with DCV did not affect the dephosphorylation of STAT3 in either cell line (Fig. 3e, f). Importantly, the tyrosine phosphatase inhibitor sodium orthovanadate did not reverse the DCV-induced inhibition of STAT3 phosphorylation (Fig. 3g, h). In conclusion, these results suggest that the inhibitory effect of DCV on STAT3 phosphorylation did not affect its upstream components or dephosphorylation.

Michael acceptor of DCV mediates STAT3 inactivation

DCV contains two α,β-unsaturated carbonyl units, which could function as a Michael receptor to react with thiols of cysteine. To investigate whether this moiety of DCV is essential for its inhibitory effects on STAT3 signaling and cell viability, DCV was coincubated with dithiothreitol (DTT) or glutathione (GSH). DTT and GSH markedly blocked DCV-induced inhibition of STAT3 phosphorylation (Fig. 4a, b). Moreover, the DCV-induced loss of cell viability was also attenuated by DTT (Fig. 4c).

To further determine whether the carbon-carbon double bond is essential for STAT3 inhibition, we utilized CV synthesized by catalytic hydrogenation of the double bond of DCV (Fig. 4d). The results showed that DCV significantly reduced the levels of phosphorylated STAT3, while CV did not inhibit the phosphorylation of STAT3 (Fig. 4e, f). The phosphorylation of STAT3 results in STAT3 dimerization and

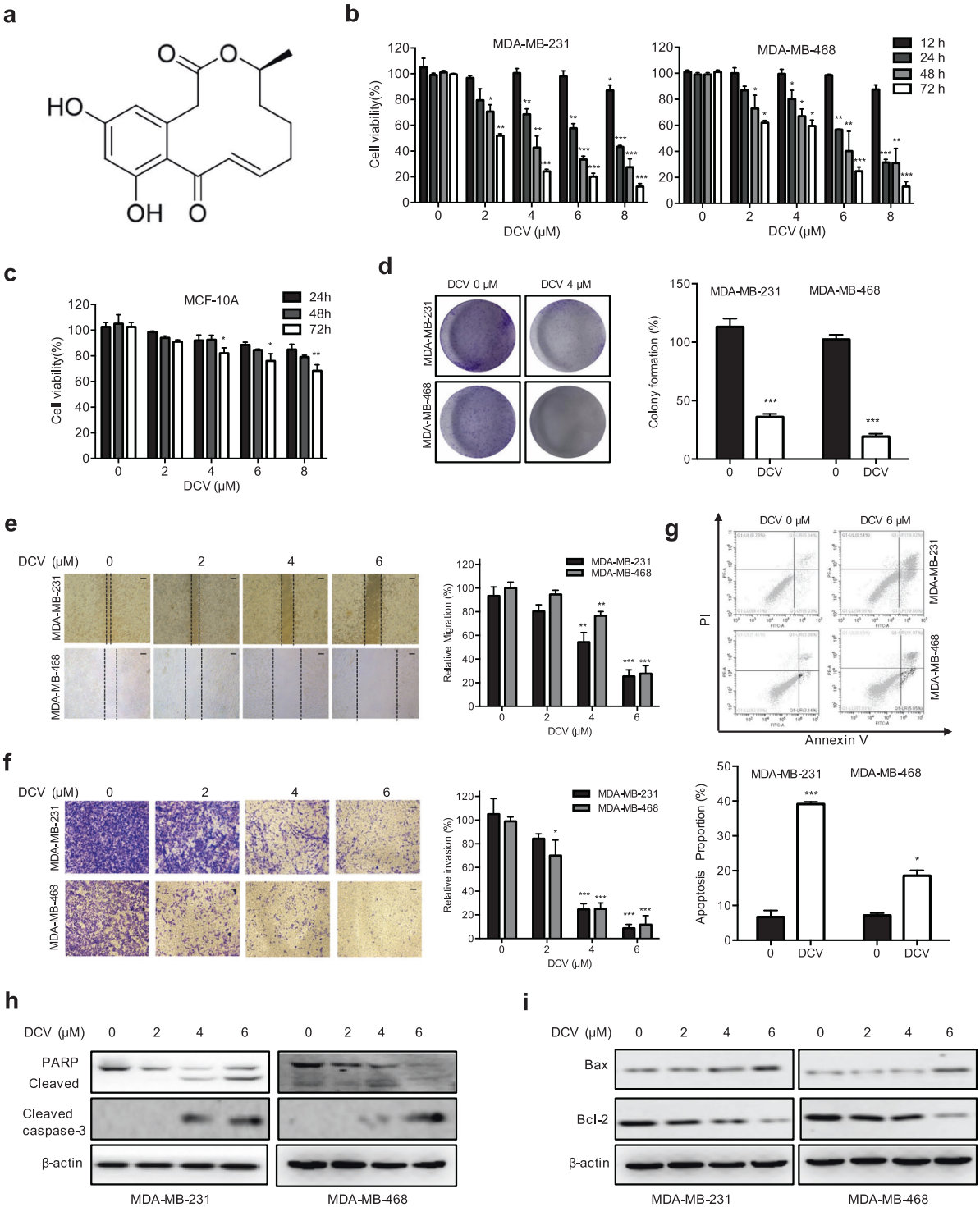

Fig. 1 Inhibitory effects of DCV on breast cancer cells. a Chemical structure of DCV. **b** MDA-MB-231 and MDA-MB-468 cells were treated with various concentrations of DCV for 12, 24, 48 and 72 h. Cell viability was analyzed by MTT assay. **c** The effect of DCV on the normal human breast epithelial cells MCF-10A. **d** The results from the colony formation assay in MDA-MB-231 and MDA-MB-468 cells after DCV treatment are shown. **e** The antimigration effect of DCV was evaluated by wound-healing assay. Confluent monolayers of MDA-MB-231 and MDA-MB-468 cells were wounded, and wound healing was monitored microscopically after 12 h of treatment with the indicated concentrations of DCV. Bar = 100 μm. **f** The invasive capacities were determined by Transwell invasion assay. MDA-MB-231 and MDA-MB-468 cells were seeded into the upper chamber of the Transwell inserts. Representative invasive cells after 12 h of incubation are shown. Bar = 100 μm. **g** MDA-MB-231 and MDA-MB-468 cells were treated with 6 μM DCV for 48 h, and the percentage of apoptotic cells was determined by labeling with annexin-V and PI followed by flow cytometry analysis. **h** MDA-MB-231 and MDA-MB-468 cells were incubated with various concentrations of DCV for 48 h. The cell lysates were analyzed for PARP and caspase-3 expression. **i** The protein expression of Bcl-2 and Bax was measured in MDA-MB-231 and MDA-MB-468 cells treated with the indicated concentrations of DCV for 48 h by Western blotting assay. The results from three independent experiments are presented. *$P < 0.05$, **$P < 0.01$ and ***$P < 0.001$ versus control.

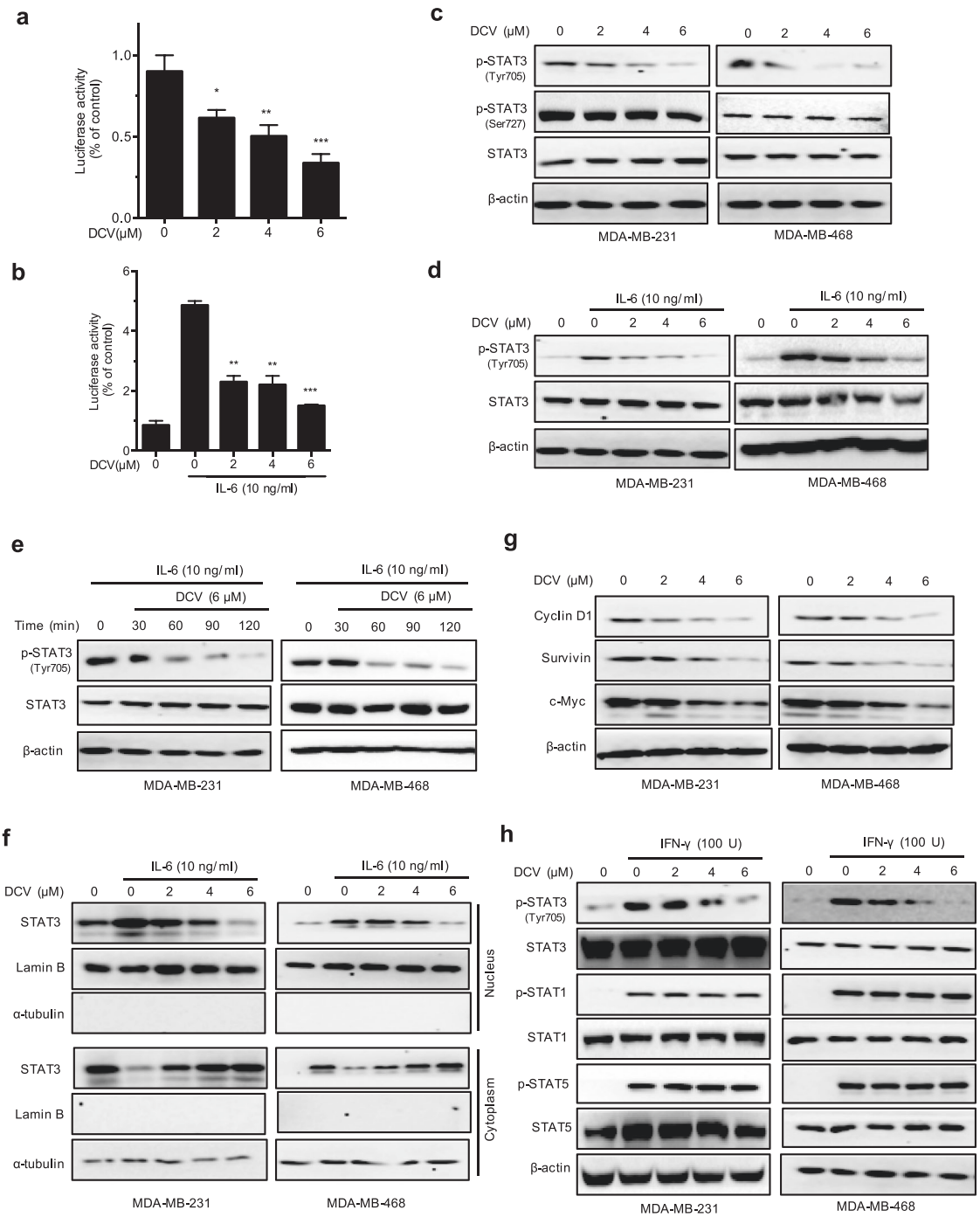

Fig. 2 DCV specifically inhibits STAT3 activation. a MDA-MB-231 cells transfected with STAT3 luciferase reporter plasmid and SV40-Renilla-Luc (as an internal control) for 24 h. Cells were then treated with DCV for 24 h, and luciferase activity was measured. **b** Luciferase assays were performed using MDA-MB-231 cells transfected with STAT3 luciferase reporter plasmid and SV40-Renilla-Luc for 24 h. The cells were then treated with DCV for 2 h, and luciferase activity was measured following stimulation with IL-6 (10 ng/mL) for 24 h. **c** Effect of DCV on constitutively active STAT3 phosphorylation. MDA-MB-231 and MDA-MB-468 cells were treated with the indicated concentrations of DCV for 2 h. The cell lysates were subjected to Western blotting to determine the Tyr705 and Ser727 phosphorylation of STAT3 and the total STAT3 protein levels. **d** Effect of DCV on inducible STAT3 activation. The cells were pretreated with the indicated concentrations of DCV for 2 h and stimulated with IL-6 (10 ng/mL) for 20 min. Cells were then lysed and subjected to Western blotting with the indicated antibodies. **e** The cells were pretreated with DCV (6 μM) for the indicated times and then stimulated with IL-6 (10 ng/mL) for 20 min. Cells were then lysed and subjected to Western blotting with the indicated antibodies. **f** MDA-MB-231 and MDA-MB-468 cells were treated with DCV for 2 h, followed by stimulation with IL-6 (10 ng/mL) for 20 min, and the cytoplasmic and nuclear extractions were subjected to Western blotting to determine the distribution of STAT3. **g** MDA-MB-231 and MDA-MB-468 cells were treated with DCV for 24 h. Cells were then lysed, and the expression of STAT3 target genes was analyzed by Western blotting with the indicated antibodies. **h** MDA-MB-231 and MDA-MB-468 cells were treated with DCV at the indicated concentrations for 2 h, followed by stimulation with IFN-γ for 15 min. Whole-cell lysates were processed for Western blot analysis using the indicated antibodies. The results from three independent experiments are presented. $^{*}P < 0.05$, $^{**}P < 0.01$ and $^{***}P < 0.001$ versus control.

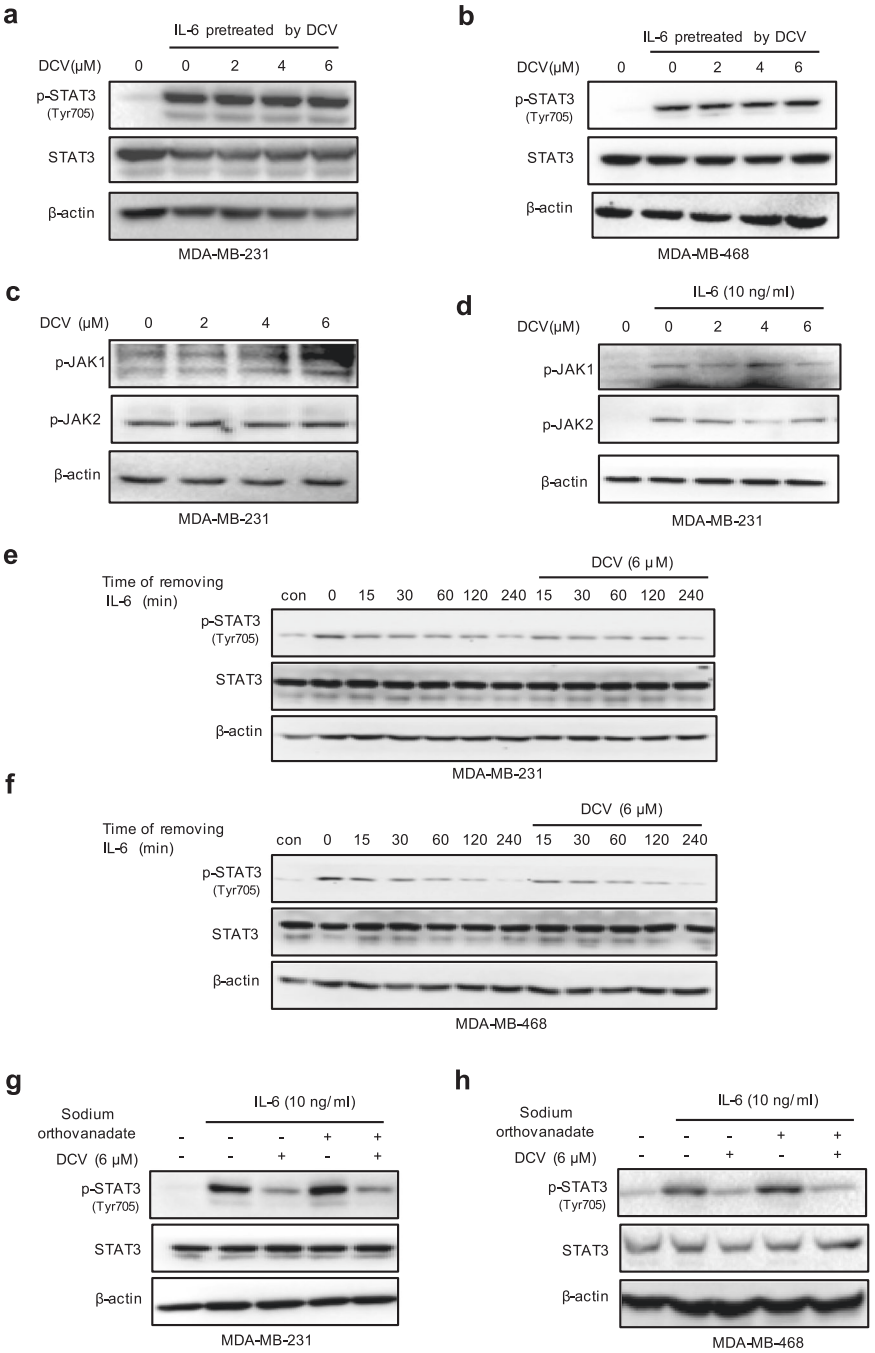

Fig. 3 DCV does not affect the upstream components of STAT3 activation. IL-6 (10 ng/mL) was incubated with DCV at the indicated concentrations in vitro for 30 min and then used to stimulate MDA-MB-231 (**a**) and MDA-MB-468 (**b**) cells for 20 min. Cells were then lysed and subjected to Western blotting with the indicated antibodies. **c** MDA-MB-231 cells were pretreated with the indicated concentrations of DCV for 2 h, and whole-cell lysates were processed for Western blot analysis using antibodies as indicated. **d** MDA-MB-231 cells were pretreated with DCV at the indicated concentrations for 2 h, followed by stimulation with IL-6 (10 ng/mL) for 20 min. Whole-cell lysates were analyzed by Western blotting using the indicated antibodies. MDA-MB-231 (**e**) and MDA-MB-468 (**f**) cells were stimulated by IL-6 (10 ng/mL) for 20 min. The media were then replaced by fresh media without IL-6 and incubated with or without DCV (6 μM) for the indicated time periods (0–240 min). Cells were lysed and subjected to Western blotting with the indicated antibodies. MDA-MB-231 (**g**) and MDA-MB-468 (**h**) cells were pretreated with sodium orthovanadate (10 μM), DCV (6 μM) or both for 2 h and then stimulated with IL-6 (10 ng/mL) for 20 min. Cells were lysed and subjected to Western blotting with the indicated antibodies.

subsequent translocation to the nucleus [37]. We next addressed whether DCV inhibited STAT3 dimerization. The results revealed that endogenous STAT3 dimerization was impaired by DCV but not CV (Fig. 4g). To further confirm that DCV disrupted STAT3 dimerization, Myc-tagged, and Flag-tagged STAT3 plasmids were transiently transfected into HEK293T cells. Coimmunoprecipitation assays indicated that DCV suppressed the dimerization of STAT3, but CV was unable to inhibit STAT3 dimerization (Fig. 4h).

Since DCV quickly inhibited the activation of STAT3, we hypothesized that DCV can directly interact with STAT3. We performed CETSA to examine whether STAT3 was engaged by DCV. As shown in Fig. 4i, STAT3 was significantly stabilized in DCV-

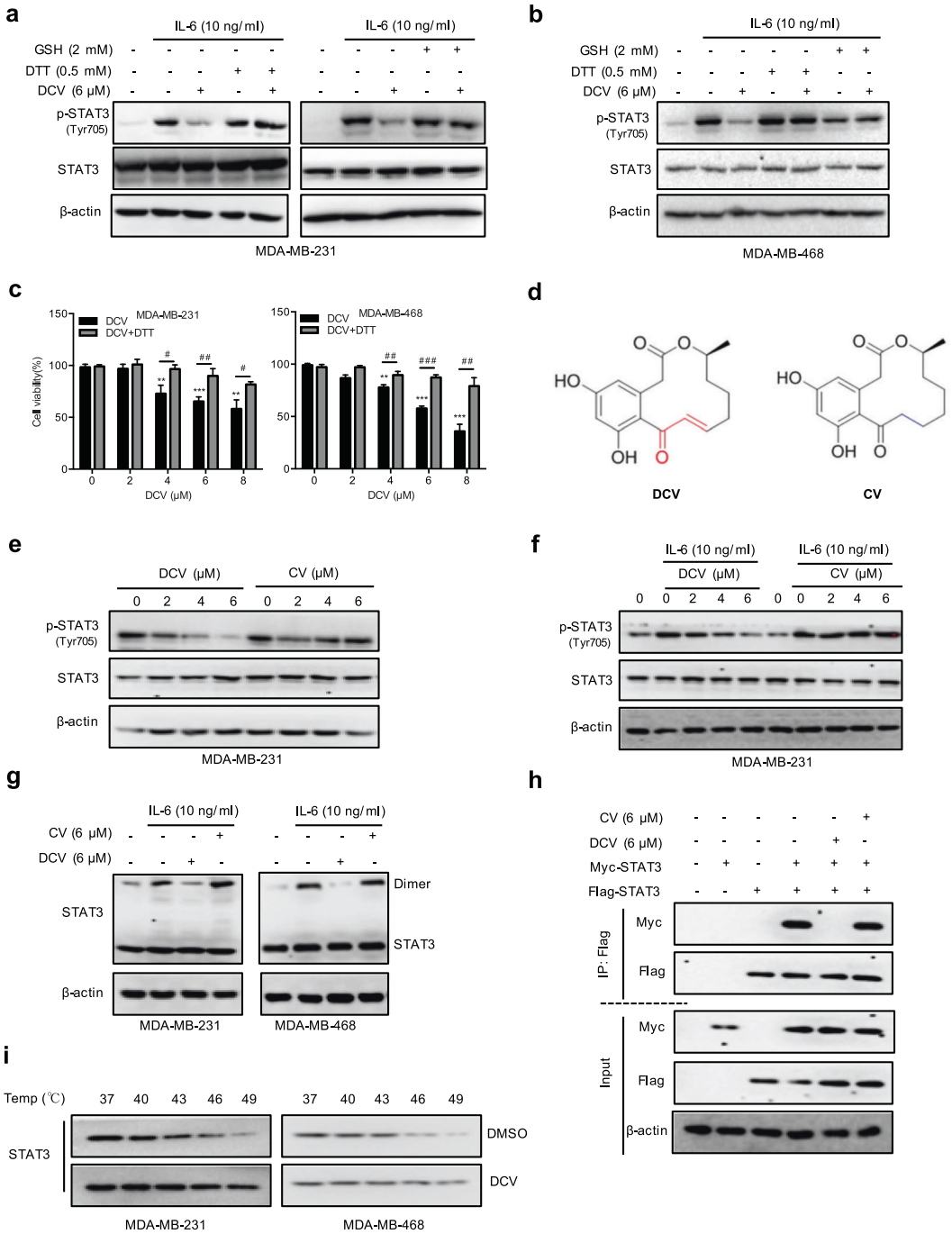

Fig. 4 Michael acceptor of DCV disturbs STAT3 dimerization. MDA-MB-231 (**a**) and MDA-MB-468 (**b**) cells were pretreated with DTT (0.5 mM), GSH (2 mM), DCV (6 μM) or their mixture (DCV and DTT/GSH were preincubated at room temperature for 30 min) for 2 h and then stimulated with IL-6 (10 ng/mL) for 20 min. Cells were lysed and subjected to Western blot analysis using antibodies as indicated. **c** MDA-MB-231 and MDA-MB-468 cells were cultured in the presence of the indicated concentrations of DCV or DCV + DTT (0.5 mM) for 24 h, and then cell viability was analyzed by MTT assay. **d** DCV has two α,β unsaturated carbonyl groups that are eliminated by curvularin (CV) by hydrogenating the double bonds. **e** MDA-MB-231 cells were incubated with the indicated concentration of DCV or CV for 2 h. The cell lysates were subjected to Western blotting to determine the p-STAT3 Tyr705 and STAT3 protein levels. **f** MDA-MB-231 cells were pretreated with the indicated concentrations of DCV or CV for 2 h and stimulated with IL-6 (10 ng/mL) for 20 min. The cell lysates were subjected to Western blotting to determine the expression of p-STAT3 Tyr705 and STAT3. **g** MDA-MB-231 and MDA-MB-468 cells were treated with 6 μM DCV and CV for 2 h, followed by stimulation with IL-6 (10 ng/mL) for 20 min. The cells were harvested, and the lysate was immunoprecipitated with STAT3 and Protein A/G agarose overnight. The level of STAT3 was detected by Western blotting. **h** HEK293T cells were transfected with Flag- and Myc-tagged STAT3 plasmids and treated with 6 μM DCV and CV for 12 h.The total lysates were subjected to immunoprecipitation with Flag beads, followed by detection with anti-Flag or Myc antibody. **i** MDA-MB-231 cells and MDA-MB-468 cells were treated with 6 μM DCV for 2 h and subsequently heated at different temperatures for 3 min. After freeze-thaw cycles for cell lysis, the soluble STAT3 protein levels were examined by Western blotting. The results from three independent experiments are presented. $^{**}P < 0.01$ and $^{***}P < 0.001$ versus control. $^{\#}P < 0.05$, $^{\#\#}P < 0.01$, $^{\#\#\#}P < 0.001$ versus DCV treatment.

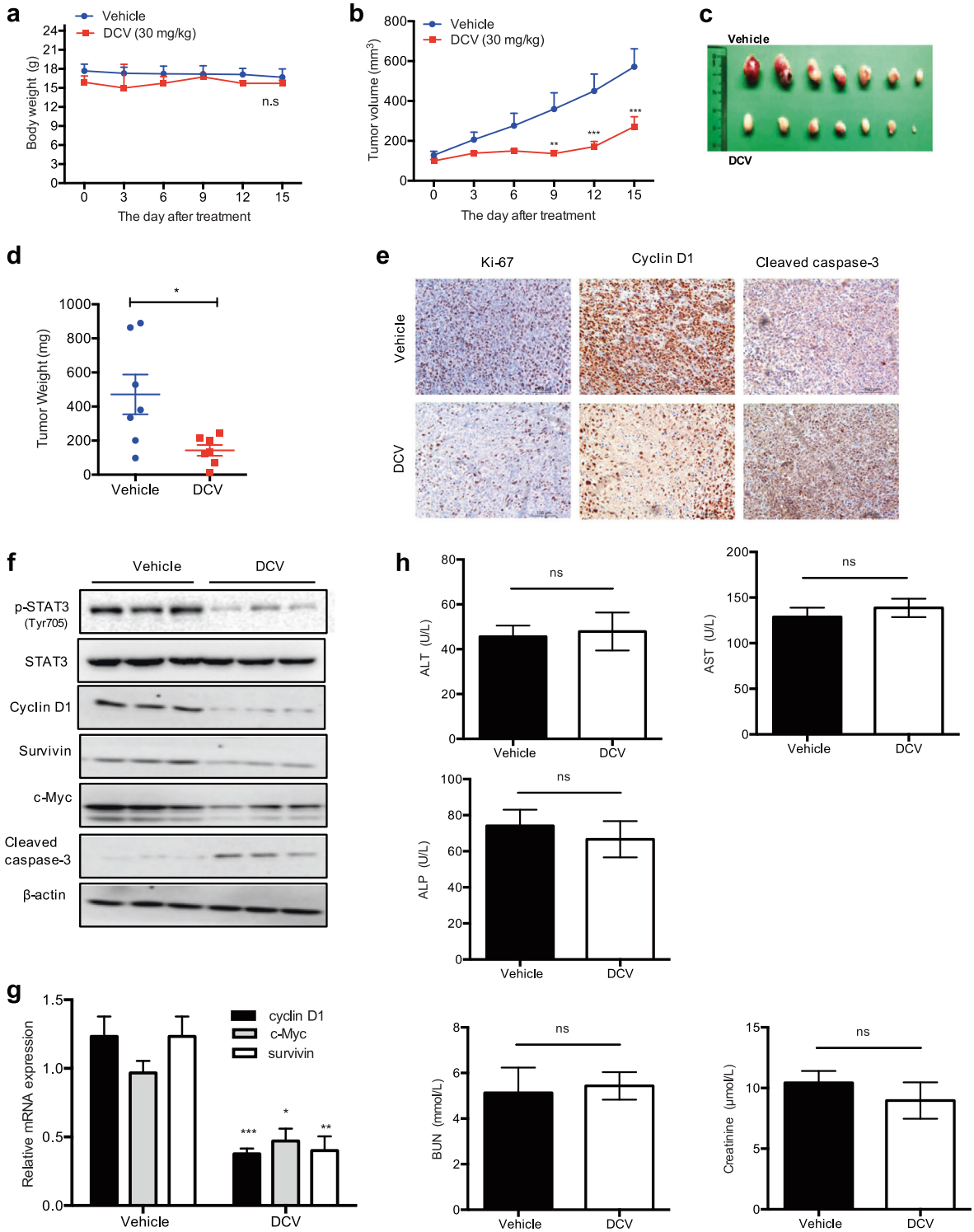

Fig. 5 DCV inhibits breast cancer growth in xenograft tumors. a MDA-MB-231 cells were subcutaneously injected into BALB/c nude mice (15 ± 2 g). Intraperitoneal treatment with vehicle or 30 mg/kg DCV was administered once every day for 14 days (7 mice/group). The body weights were calculated for the vehicle- and DCV-treated mice during the experiment. **b** The tumor volume was monitored. **c** At the end of the experiment, the tumors were excised. Images of resected human breast tumors taken for the vehicle and DCV treatment groups. **d** The tumors were weighed. **e** Representative images of Ki67, cleaved caspase-3 and Cyclin D1 immunostaining in vehicle- and DCV-treated tumor tissues. Bar = 100 μm. **f** The tumor tissues were homogenized and lysed in RIPA buffer, and the expression of p-STAT3 Tyr705, STAT3, Cyclin D1, survivin, c-Myc, and cleaved caspase-3 was detected by Western blotting. **g** Real-time RT-PCR assay was performed to assess the expression of Cyclin D1, c-Myc and survivin. **h** Nude BALB/c mice were administered vehicle or DCV (30 mg·kg^{-1}·d^{-1}) by intraperitoneal injection once every day for 14 days. All animals were sacrificed after collecting blood samples and tissues. The results of plasma biochemical tests for ALT, AST, ALP, BUN, and creatinine in vehicle- or DCV-treated mice. *$P < 0.05$, **$P < 0.01$ and ***$P < 0.001$ versus vehicle treatment.

treated cells, suggesting the direct engagement of DCV with STAT3. Collectively, these results indicate that the Michael acceptor of DCV is responsible for the inhibition of STAT3 activation and function.

DCV suppresses breast cancer growth in xenograft tumors

To determine whether DCV inhibited tumors in vivo, MDA-MB-231 cells were subcutaneously injected into the right flanks of nude mice. Tumor-bearing mice were treated with DCV at 30 $mg{\cdot}kg^{-1}{\cdot}d^{-1}$ for 14 days. We found no significant differences in body weight after DCV treatment, suggesting that DCV had no obvious toxic side effects (Fig. 5a). However, tumor size and tumor weight were markedly reduced in DCV-treated mice compared with vehicle-treated mice (Fig. 5b–d).

To further confirm the in vitro results, we analyzed the expression of the indicated proteins in tumor tissues by immunohistochemistry and Western blot assays. A marked reduction in the proliferation biomarkers Ki67 and Cyclin D1 was observed in DCV-treated tumor tissues (Fig. 5e). To determine whether the lower proliferation in DCV-treated tumor tissues is linked with apoptosis, we measured apoptosis by detecting cleaved caspase-3. DCV-treated tumor tissues showed more caspase-3-positive cells than vehicle-treated tumor tissues (Fig. 5e). These results were further strengthened by Western blotting analysis (Fig. 5f). Furthermore, the level of phospho-STAT3 was markedly decreased in DCV-treated tumor tissues compared with vehicle-treated tumor tissues (Fig. 5f). Additionally, DCV-treated tumor tissues showed a marked reduction in the STAT3 target genes Cyclin D1, survivin, and c-Myc (Fig. 5f, g).

To evaluate the safety of DCV in vivo, we detected its toxicity in blood, heart, liver, spleen, and kidney after DCV treatment. No notable differences in blood biochemical parameters (ALT, AST, ALP, BUN, and creatinine) were observed between the vehicle and DCV-treated groups (Fig. 5h). Taken together, these results demonstrate that DCV suppresses tumor growth and STAT3 activation in vivo.

DISCUSSION

Constitutively activated STAT3 contributes to tumor progression and development in cancers, and STAT3 might become an attractive molecular target for antitumor drug development [25]. Some natural products and derivatives, such as curcumin [38], resveratrol [39], Eriocalyxin B [40], have gained much attention because of their safety, efficacy, and availability. DCV, a natural-product from a marine-derived fungus, has been found to exert anti-inflammatory and antitumor effects [26–30]. However, the molecular mechanism of DCV in breast cancer remains unclear. Herein, we demonstrated that DCV acted as a potent STAT3 inhibitor. Further study suggested that the α,β-unsaturated carbonyl unit of DCV was essential for its inhibitory effects on STAT3 activation because a reduction in the carbon-carbon double bond abrogated its inhibitory activity on STAT3. In addition, in vivo models also revealed the anticancer efficacy of DCV, which is mediated by its inhibition of STAT3 activation; in addition, DCV had no obvious side effects.

Ligands and tyrosine kinases are considered crucial inducers of STAT3 dimerization [37, 41]. Our results indicated that DCV did not affect the upstream pathway components or the dephosphorylation of STAT3. Moreover, DCV also did not inhibit STAT3 phosphorylation at Ser727 and had no effect on STAT1 or STAT5 phosphorylation. Thus, we suggest a possible direct interaction between DCV and STAT3. DCV contains an electrophilic α,β-unsaturated carbonyl moiety that tends to react with a variety of electron donors. Cysteine thiol residues ubiquitously present in cellular proteins can be covalently modified. Many studies suggest that electrophilic attack is a critical biological process [40, 42, 43]. Our previous study reported that DCV exhibited anticancer activity based on the α, β-unsaturated carbonyl moiety [30]. In the present study, the results indicated that the thiol-reducing agents DTT and GSH reversed the DCV-mediated inhibition of STAT3 phosphorylation and loss of cell viability. In line with this finding, DCV suppressed STAT3 phosphorylation and dimerization, while CV, which lacks an α, β-unsaturated carbonyl moiety, was incapable of inhibiting STAT3 activation. Furthermore, we found direct engagement of DCV with STAT3 by CETSA. Therefore, our results indicated that the direct modification of STAT3 by DCV prevented STAT3 phosphorylation and dimerization and subsequently suppressed STAT3 signaling.

Several reports have demonstrated the antitumor activities of DCV [29, 30]. In line with this, our data indicated that DCV significantly inhibited breast cancer cell growth and had little cytotoxicity in normal human mammary epithelial cells. One of the important findings of our work is that DCV displayed satisfactory therapeutic effects in vivo. We found that DCV treatment significantly inhibited breast cancer tumor growth. More importantly, STAT3 activation was also inhibited by DCV treatment compared with vehicle treatment, suggesting that DCV is a promising anti-breast cancer agent for clinical trials.

In conclusion, our studies demonstrated that DCV exhibited inhibitory potential by directly engaging with STAT3, leading to inactivation of STAT3 signaling. In addition, we found that DCV inhibited tumor growth by inactivating STAT3 in vivo with no obvious side effects. Therefore, our findings imply that DCV may be useful in breast cancer prevention and treatment.

ACKNOWLEDGEMENTS

This project was supported by research funds from the National Natural Science Foundation of China (No. 81502548, 81902852), the Natural Science Foundation of Hubei Provincial Department of Education (D20182101), the Foundation of Health Commission of Hubei Province (WJ2019M053), the Biomedical Research Foundation, Hubei University of Medicine (HBMUPI201809), the Foundation for Innovative Research Team of Institute of Medicine and Nursing, Hubei University of Medicine (2017YHKT01), Faculty Development Grants from Hubei University of Medicine (2018QDJZR06), the Open Project of Hubei Key Laboratory of Embryonic Stem Cell Research (2020ESOF008) and Wudang Local Chinese Medicine Research of Hubei University of Medicine (WDCM2019006), and Innovative Research Program for Graduates of Hubei University of Medicine (YC2019010, YC2020005).

AUTHOR CONTRIBUTIONS

QZ and XJY conceived and planned the experiments; QZ, YB, JZ, XL, and ZSD performed the experiments; QZ, YB, JZ, XL, JG, YXL, LRP, YT, ZSD and XJY analyzed the data; QZ, ZSD, and XJY wrote the manuscript.

ADDITIONAL INFORMATION

The online version of this article (https://doi.org/10.1038/s41401-020-0499-y) contains supplementary material, which is available to authorized users.

Competing interests: The authors declare no competing interests.

REFERENCES

1. Siegel RL, Miller KD, Jemal A. Cancer statistics, 2020. CA Cancer J Clin. 2020;70:7–30.
2. Chen W, Zheng R, Baade PD, Zhang S, Zeng H, Bray F, et al. Cancer statistics in China, 2015. CA Cancer J Clin. 2016;66:115–32.
3. Dean M, Fojo T, Bates S. Tumour stem cells and drug resistance. Nat Rev Cancer. 2005;5:275–84.
4. Bange J, Zwick E, Ullrich A. Molecular targets for breast cancer therapy and prevention. Nat Med. 2001;7:548–52.
5. Aydiner A. Meta-analysis of breast cancer outcome and toxicity in adjuvant trials of aromatase inhibitors in postmenopausal women. Breast. 2013;22:121–9.
6. Dent R, Trudeau M, Pritchard KI, Hanna WM, Kahn HK, Sawka CA, et al. Triple-negative breast cancer: clinical features and patterns of recurrence. Clin Cancer Res. 2007;13:4429–34.
7. Bromberg J. Signal transducers and activators of transcription as regulators of growth, apoptosis and breast development. Breast Cancer Res. 2000;2:86–90.

8. Ortmann RA, Cheng T, Visconti R, Frucht DM, O'Shea JJ. Janus kinases and signal transducers and activators of transcription: their roles in cytokine signaling, development and immunoregulation. Arthritis Res. 2000;2:16–32.
9. Aggarwal BB, Sethi G, Ahn KS, Sandur SK, Pandey MK, Kunnumakkara AB, et al. Targeting signal-transducer-and-activator-of-transcription-3 for prevention and therapy of cancer - Modern target but ancient solution. Ann N Y Acad Sci. 2006;1091:151–69.
10. Chung JK, Uchida E, Grammer TC, Blenis J. STAT3 serine phosphorylation by ERK-dependent and -independent pathways negatively modulates its tyrosine phosphorylation. Mol Cell Biol. 1997;17:6508–16.
11. Hemmann U, Gerhartz C, Heesel B, Sasse J, Kurapkat G, Grotzinger J, et al. Differential activation of acute phase response factor/Stat3 and Stat1 via the cytoplasmic domain of the interleukin 6 signal transducer gp130: II. Src homology SH2 domains define the specificity of STAT factor activation. J Biol Chem. 1996;271:12999–3007.
12. Yu H, Lee H, Herrmann A, Buettner R, Jove R. Revisiting STAT3 signalling in cancer: new and unexpected biological functions. Nat Rev Cancer. 2014;14:736–46.
13. Zhuang SG. Regulation of STAT signaling by acetylation. Cell Signal. 2013;25:1924–31.
14. Banerjee K, Resat H. Constitutive activation of STAT3 in breast cancer cells: A review. Int J Cancer. 2016;138:2570–8.
15. Chang RX, Song LL, Xu Y, Wu YJ, Dai C, Wang XY, et al. Loss of Wwox drives metastasis in triple-negative breast cancer by JAK2/STAT3 axis. Nat Commun. 2018;9:3486.
16. Xie Q, Yang ZJ, Huang XM, Zhang ZK, Li JB, Ju JH, et al. Ilamycin C induces apoptosis and inhibits migration and invasion in triple-negative breast cancer by suppressing IL-6/STAT3 pathway. J Hematol Oncol. 2019;12:60.
17. Kim MS, Lee HS, Kim YJ, Lee DY, Kang SG, Jin W. MEST induces Twist-1-mediated EMT through STAT3 activation in breast cancers. Cell Death Differ. 2019;26:2594–606.
18. Doherty MR, Parvani JG, Tamagno I, Junk DJ, Bryson BL, Cheon HJ, et al. The opposing effects of interferon-beta and oncostatin-M as regulators of cancer stem cell plasticity in triple-negative breast cancer. Breast Cancer Res. 2019;21:54.
19. Tzeng YDT, Liu PF, Li JY, Liu LF, Kuo SY, Hsieh CW, et al. Kinome-wide siRNA screening identifies Src-enhanced resistance of chemotherapeutic drugs in triple-negative breast cancer cells. Front Pharmacol. 2018;9:1285.
20. Wang TY, Fahrmann JF, Lee H, Li YJ, Tripathi SC, Yue CY, et al. JAK/STAT3-regulated fatty acid beta-oxidation is critical for breast cancer stem cell self-renewal and chemoresistance. Cell Metab. 2018;27:136–50.
21. Buettner R, Mora LB, Jove R. Activated STAT signaling in human tumors provides novel molecular targets for therapeutic intervention. Clin Cancer Res. 2002;8:945–54.
22. Zhang XL, Yue PB, Page BDG, Li TS, Zhao W, Namanja AT, et al. Orally bioavailable small-molecule inhibitor of transcription factor Stat3 regresses human breast and lung cancer xenografts. Proc Natl Acad Sci U S A. 2012;109:9623–8.
23. Liu CY, Tseng LM, Su JC, Chang KC, Chu PY, Tai WT, et al. Novel sorafenib analogues induce apoptosis through SHP-1 dependent STAT3 inactivation in human breast cancer cells. Breast Cancer Res. 2013;15:R63.
24. Yu H, Jove R. The stats of cancer - new molecular targets come of age. Nat Rev Cancer. 2004;4:97–105.
25. Ma JH, Qin L, Li X. Role of STAT3 signaling pathway in breast cancer. Cell Commun Signal. 2020;18:33. https://doi.org/10.1186/s12964-020-0527-z.
26. Deng ZS, Deng AP, Luo D, Gong DC, Zou K, Peng Y, et al. Biotransformation of (-)-(10E,15S)-10,11-dehydrocurvularin. Nat Prod Commun. 2015;10:1277–8.
27. Xu YQ, Espinosa-Artiles P, Schubert V, Xu YM, Zhang W, Lin M, et al. Characterization of the biosynthetic genes for 10,11-dehydrocurvularin, a heat shock response-modulating anticancer fungal polyketide from *Aspergillus terreus*. Appl Environ Micro. 2013;79:2038–47.
28. Ha TM, Ko W, Lee SJ, Kim YC, Son JY, Sohn JH, et al. Anti-inflammatory effects of curvularin-type metabolites from a marine-derived fungal strain penicillium sp SF-5859 in lipopolysaccharide-induced RAW264.7 macrophages. Mar Drugs. 2017;15:282.
29. Rudolph K, Serwe A, Erkel G. Inhibition of TGF-beta signaling by the fungal lactones (*S*)-curvularin, dehydrocurvularin, oxacyclododecindione and galiellalactone. Cytokine. 2013;61:285–96.
30. Deng ZS, Wong NK, Guo ZY, Zou K, Xiao YL, Zhou YQ. Dehydrocurvularin is a potent antineoplastic agent irreversibly blocking ATP-citrate lyase: evidence from chemoproteomics. Chem Commun (Camb). 2019;55:4194–7.
31. Zhao Q, Liu YX, Zhong J, Bi Y, Liu YQ, Ren ZT, et al. Pristimerin induces apoptosis and autophagy via activation of ROS/ASK1/JNK pathway in human breast cancer in vitro and in vivo. Cell Death Discov. 2019;5:125.
32. Zhao Q, Bi Y, Zhong J, Ren Z, Liu Y, Jia J, et al. Pristimerin suppresses colorectal cancer through inhibiting inflammatory responses and Wnt/beta-catenin signaling. Toxicol Appl Pharmacol. 2020;386:114813. https://doi.org/10.1016/j.taap.2019.114813.
33. Cheng X, Liu YQ, Wang GZ, Yang LN, Lu YZ, Li XC, et al. Proteomic identification of the oncoprotein STAT3 as a target of a novel Skp1 inhibitor. Oncotarget. 2017;8:2681–93.
34. Real PJ, Sierra A, de Juan A, Segovia JC, Lopez-Vega JM, Fernandez-Luna JL. Resistance to chemotherapy via Stat3-dependent overexpression of Bcl-2 in metastatic breast cancer cells. Oncogene. 2002;21:7611–8.
35. Ernst M, Najdovska M, Grail D, Lundgren-May T, Buchert M, Tye H, et al. STAT3 and STAT1 mediate IL-11-dependent and inflammation-associated gastric tumorigenesis in gp130 receptor mutant mice. J Clin Invest. 2008;118:1727–38.
36. Paukku K, Silvennoinen O. STATs as critical mediators of signal transduction and transcription: lessons learned from STAT5. Cytokine Growth Factor Rev. 2004;15:435–55.
37. Yu H, Kortylewski M, Pardoll D. Crosstalk between cancer and immune cells: role of STAT3 in the tumour microenvironment. Nat Rev Immunol. 2007;7:41–51.
38. Bharti AC, Donato N, Aggarwal BB. Curcurnin (diferuloylmethane) inhibits constitutive and IL-6-inducible STAT3 phosphorylation in human multiple myeloma cells. J Immunol. 2003;171:3863–71.
39. Kotha A, Sekharam M, Cilenti L, Siddiquee K, Khaled A, Zervos AS, et al. Resveratrol inhibits Src and Stat3 signaling and induces the apoptosis of malignant cells containing activated Stat3 protein. Mol Cancer Ther. 2006;5:621–9.
40. Yu XK, He L, Cao P, Yu Q. Eriocalyxin B inhibits STAT3 signaling by covalently targeting STAT3 and blocking phosphorylation and activation of STAT3. PLoS ONE. 2015;10:e0128406.
41. Yu H, Pardoll D, Jove R. STATs in cancer inflammation and immunity: a leading role for STAT3. Nat Rev Cancer. 2009;9:798–809.
42. Gersch M, Kreuzer J, Sieber SA. Electrophilic natural products and their biological targets. Nat Prod Rep. 2012;29:659–82.
43. Hahn YI, Kim SJ, Choi BY, Cho KC, Bandu R, Kim KP, et al. Curcumin interacts directly with the Cysteine 259 residue of STAT3 and induces apoptosis in H-Ras transformed human mammary epithelial cells. Sci Rep. 2018;8:6409. https://doi.org/10.1038/s41598-018-23840-2.